s-wave superconductivity with orbital-dependent sign change in checkerboard models of iron-based superconductors

Xiaoli Lu, Chen Fang, Wei-Feng Tsai, Yongjin Jiang, and Jiangping Hu

Phys. Rev. B **85**, 054505 — Published 14 February 2012

DOI: 10.1103/PhysRevB.85.054505

S-wave superconductivity with orbital dependent sign change in the checkerboard models of iron-based superconductors

Xiaoli Lu,[1,2] Chen Fang,[2] Wei-Feng Tsai,[3,4] Yongjin Jiang,[1,2] and Jiangping Hu[5,2,*]

[1] *Center for Statistical and Theoretical Condensed Matter Physics, and Department of Physics, Zhejiang Normal University, Jinhua 321004, China*
[2] *Department of Physics, Purdue University, West Lafayette, Indiana 47907, USA*
[3] *Institute for Solid State Physics, University of Tokyo, Kashiwa 277-8581, Japan*
[4] *Department of Physics, National Sun Yat-sen University, Kaohsiung 804, Taiwan, Republic of China*
[5] *Beijing National Laboratory for Condensed Matter Physics, Institute of Physics, Chinese Academy of Sciences, Beijing 100080, China*

We study three different multi-orbital models for iron-based superconductors (iron-SCs) in the solvable limit of weakly coupled square plaquettes. The strongest superconducting (SC) pairing is in the A_{1g} s-wave channel and its development is correlated with the emergence of the next-nearest-neighbour antiferromagnetism (NNN-AFM). Increasing the NNN-AFM interactions can drastically enhance the s-wave SC pairing. For the models with more than two orbitals, our study suggests that the signs of the intra-orbital pairing superconducting order of the d_{xy} and the d_{xz} (or d_{yz}) orbitals must be *opposite*. Such sign difference stems from the intrinsic symmetry properties of inter-orbital hoppings and might, in the homogeneous case, lead to the sign-change of the SC orders between the hole Fermi pockets at the Γ and M points in the unfolded Brillouin zone.

I. INTRODUCTION

Since the iron-based superconductors were discovered two years ago[1], the relation between these superconductors and the high-T_c cuprates has been a central focus of researches. It is highly debated that whether the iron-based superconductors belong to the same category of strongly correlated electron systems as the cuprates. Models based on both strong coupling[2–9] and weak coupling[10–16] approaches have been applied to understand the properties of these materials and their relation to the curpates.

A strongly correlated electron system exhibits strong "locality" in its physical properties. For instance, both magnetism and superconductivity in the cuprates could be described locally in real space. The magnetism of the parent cuprate compounds is well described by the Heisenberg model with the nearest-neighbor (NN) antiferromagnetic (AFM) exchange couplings. The d-wave superconductivity with the symmetry form factor in reciprocal space, $\cos k_x - \cos k_y$,[17] corresponds to short-range SC pairings between two electrons at NN copper sites. With such a short pairing length, we can study essential physics in a four-site cluster to extract key elements for low-energy effective models[18–21].

It is clear that iron-based superconductors are more itinerant than cuprates. The parent compounds of iron-pnictides are metallic rather than insulating. So far, the majority of theories for the pairing symmetry of iron-based superconductors are based on weak coupling approaches[10–16]. Although there are discrepancies, the theories based on these approaches have reached a broad consensus regarding the pairing symmetries in iron-based superconductors: for optimally hole doped iron-pnictides, for example, $Ba_{0.6}K_{0.4}Fe_2As_2$, an extended s-wave pairing symmetry, called $s^{\pm}$, is favored[10], as a result of repulsive interband interactions and nesting between the hole and electron pockets. However, in the weak coupling approach, the $s^{\pm}$ pairing is not robust. For extremely hole-doped materials, such as KFe_2As_2, and extremely electron-doped materials, such as KFe_2Se_2, a d-wave pairing symmetry is stronger than s-wave pairing[22–24].

Intriguingly, recent experiments in the iron-SCs suggest that both magnetism and superconductivity display many locality behaviors as well. Neutron scattering experiments demonstrate that the magnetism in many parent compounds of iron-SCs can be described well by the Heisenberg model with the NN and the NNN-AFM exchange couplings between iron spins[25–27]. In addition, angle resolved photoemission spectroscopy (ARPES) experiments show that the SC gaps can be fitted to a single $\cos k_x \cos k_y$ functional form in reciprocal space[28–30]. Regarding the fact that the iron-SCs are complicated multi-orbital systems, these experimental results are compelling evidence to support that the SC pairing stems from local interactions because the functional form, viewed in real space, corresponds to pairings between two electrons at NNN iron sites. Moreover, the recently discovered ironchalcogenide, KFe_2Se_2, has a magnetically ordered insulating state[31] in which electron-electron correlation may play an important role. Therefore, it is natural to ask whether the physics of the iron-SCs can also be understood in a checkerboard-like system studied in Ref. 19 in which local physics can be solved exactly.

In this paper, we present results for three different checkerboard tight-binding models as shown in Fig. 1 for the iron-SCs which are constructed using two[32], three[33], and four orbitals[34], respectively. By exactly solving the 2×2 plaquette problem, we show the comprehensive phase diagrams of the models in the limit of weakly coupled plaquettes, by varying intra-orbital onsite interaction U, inter-orbital onsite interaction U', Hund's cou-

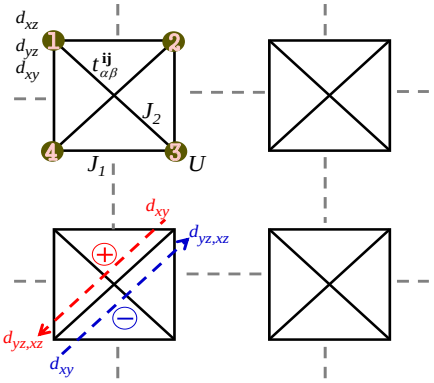

FIG. 1: The sketch of the checkerboard models. The hopping signs between d_{xy} and $d_{xz(yz)}$ orbitals are indicated.

pling J_H, as well as the NN(NNN)-AFM coupling $J_{1(2)}$. Here we allow $J_{1,2}$ to be independent parameters because they, in principle, are generated by superexchange mechanism via As atoms. In all of the models, we obtain that the leading SC order is always in the A_{1g} s-wave pairing channel. Most remarkably, this study also shows that the superconductivity and magnetism are orbital-selective in the three- and four-orbital models: First, in the three-orbital model, the short-range antiferromagnetic correlation is more pronounced in the d_{xy} orbital while the superconductivity more pronounced in the d_{xz} and d_{yz} orbitals. Second, in both three- and four-orbital models, the signs of the intra-orbital pairing order parameters of the d_{xy} and the d_{xz} (or d_{yz}) orbitals are opposite. The sign difference originates from the intrinsic symmetry of the inter-orbital hopping between d_{xy} and $d_{xz(yz)}$[36]. This feature could result in a new sign-change of the SC orders between the hole Fermi pockets at the Γ and M points in the unfolded Brillouin zone. In particular, both of the results mentioned above may not be easily explained by the Fermi surface nesting properties and hence should be attributed to the strong correlations in the models.

II. MODEL AND METHOD

A generic Hamiltonian of iron-SCs can be written as $H = H_0 + H_I$, where H_0 is the kinetic energy of the d-electrons on iron sites and H_I includes the interactions between them. Explicitly, H_0 is given by

$$H_0 = \sum_{\mathbf{i},\mathbf{j},\sigma}\sum_{\alpha,\beta}(t^{\mathbf{ij}}_{\alpha\beta} + \epsilon_\alpha\delta_{\alpha\beta})d^\dagger_{\mathbf{i},\alpha,\sigma}d_{\mathbf{j},\beta,\sigma} + H.c. \quad (2.1)$$

where α,β are orbital indices; $\mathbf{i},\mathbf{j}$ label the sites and σ is the spin index. H_I can be written as $H_I = \sum_{\mathbf{i}} H_{Io}(\mathbf{i}) + H_{Ie}$. $H_{Io}(\mathbf{i})$ is the onsite interaction, given by,

$$\begin{aligned} H_{Io}(\mathbf{i}) &= U\sum_{\alpha} n_{\mathbf{i},\alpha,\uparrow}n_{\mathbf{i},\alpha,\downarrow} + \sum_{\alpha\neq\beta}[\frac{U'}{2}n_{\mathbf{i},\alpha}n_{\mathbf{i},\beta} - \frac{J_H}{2}S_{\mathbf{i}\alpha}S_{\mathbf{i}\beta}] \\ &+ J\sum_{\alpha\neq\beta} d^\dagger_{\mathbf{i},\alpha,\uparrow}d^\dagger_{\mathbf{i},\alpha,\downarrow}d_{\mathbf{i},\beta,\downarrow}d_{\mathbf{i},\beta,\uparrow}, \end{aligned} \quad (2.2)$$

with U, U', J_H, and $J(=J_H)$ denoting intra-orbital repulsion, inter-orbital repulsion, ferromagnetic Hund's coupling, and inter-orbital pair hopping, respectively.

H_{Ie} includes interactions between different sites. In this paper, we consider the NN (denoted by single angular bracket) magnetic exchange coupling J_1 and NNN (denoted by double angular bracket) magnetic exchange coupling J_2, both of which are generated by the superexchange mechanism through As atoms as shown in Ref. 3. The explicit form of H_{Ie} reads

$$H_{Ie} = \sum_{\langle\mathbf{i},\mathbf{j}\rangle}\sum_{\alpha,\beta} J_1\mathbf{S}_{\mathbf{i},\alpha}\cdot\mathbf{S}_{\mathbf{j},\beta} + \sum_{\langle\langle\mathbf{i},\mathbf{j}\rangle\rangle}\sum_{\alpha,\beta} J_2\mathbf{S}_{\mathbf{i},\alpha}\cdot\mathbf{S}_{\mathbf{j},\beta}. \quad (2.3)$$

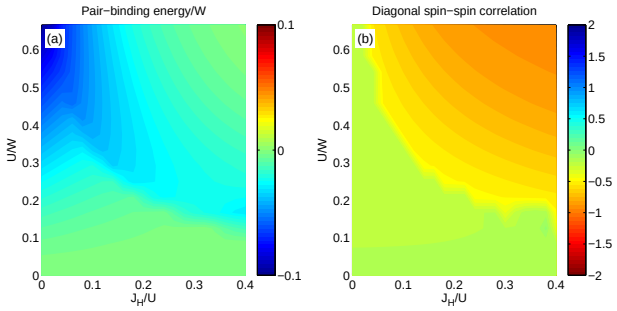

FIG. 2: The pair-binding energy (a) and the diagonal spin-spin correlations (b) for a 2×2 plaquette in the two-orbital model are plotted as functions of U/W and J_H/U without exchange coupling J_1 and J_2.

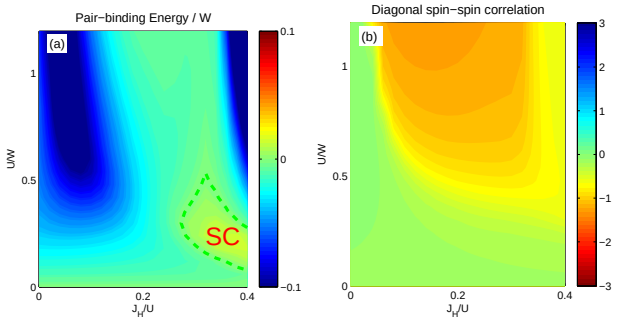

FIG. 3: The pair-binding energy (a) and the diagonal spin-spin correlations (b) for 2×2 plaquette in the three-orbital model are plotted as functions of U/W and J_H/U without exchange coupling J_1 and J_2. The dotted lines in (a) enclose the regions with positive pair-binding energy, suggesting a SC phase.

Different tight-binding models have been proposed to describe the band structures of iron-SCs. In this study,

we take three different models: a two-orbital model given in Ref.32, a three-orbital model given in Ref.33, and a four-orbital model in Ref.34. The tight-binding parameters of the models can be found in the above references. Additionally, we have also tried a different four-orbital models reduced from the five-orbital models constructed in Ref.11. All of the models capture the basic band structures of iron-SCs. In fact, the major results reported below are consistent in all of these models.

The checkerboard models are defined on the lattice shown in Fig. 1, with the inter-plaquette hopping amplitudes $\tau^{\mathbf{ij}}_{\alpha\beta}$ and exchange couplings $\mathcal{J}_{1,2}$ much smaller than intra-plaquette parameters, $t^{\mathbf{ij}}_{\alpha\beta}$ and $J_{1,2}$. A four-site plaquette can be diagonalized exactly, though one may necessarily resort to the numerical exact diagonalization (ED) due to its multi-orbital complexity. Consequently, we can determine the pair-binding energy $E_p = 2E(1) - E(0) - E(2)$, where $E(Q)$ is the ground-state energy for a given Q, the number of doped holes in an "undoped" reference state. In particular, $E_p > 0$ indicates an effective attraction between doped holes, i.e., a local pairing of two holes. At generic doping, we consider the case $0 \leq \{\tau^{\mathbf{ij}}_{\alpha\beta}, \mathcal{J}_{1,2}\} \ll E_p \ll \{t^{\mathbf{ij}}_{\alpha\beta}, J_{1,2}\}$, which allows us to obtain a controlled perturbation expansion of the full Hamiltonian in terms of small inter-plaquette parameters. Second order perturbation gives us an effective theory describing interacting bosons ($Q = 2$ states) with effective hopping integrals and short-ranged density-density interactions of order τ^2/E_p on the effective lattice. Furthermore, it can be proved that the ground state of this effective theory enters superfluidity at $T = 0$[35], except at special doping percentages. Thus, in this study we do not show explicitly the effective coupling strength as a function of inter-plaquette parameters, but rather solve the 2×2 plaquette problem with open boundary conditions by numerical exact diagonalization. Since the effective hopping integrals are generically non-zero, the positiveness of E_p can be used as an economic way to identify SC phase at generic doping on the checkerboard-like lattice as long as E_p is still larger than any one of the inter-plaquette parameters.

III. NUMERICAL RESULTS

A. In absence of J_1 and J_2

We summarize the main results for the two-orbital and three-orbital models without magnetic exchange coupling J_1 or J_2 in Figs. 2 and 3. Note that the parent compounds in a three orbital model have a nominal filling of 2/3, instead of 1/2 filling in two- and four-orbital models. In Fig. 2 and Fig. 3, we plot the pair-binding energy and the diagonal (NNN) spin-spin correlation function as a function of U/W and J_H/U with U' satisfying the $SU(2)$ symmetry condition $U' = U - 2.5J_H$ and W being the bandwidth. As shown in Fig. 2, there is no SC phase in the physically meaningful parameter region in two-orbital model. While in Fig. 3, there is a very small region (circled by the dashed line) where the SC state is favored and this region is located within the region the NNN-AFM is developed. The diagonal spin-spin correlation in two-orbital is very similar to the result in three-orbital model. It tells us that the diagonal spins are antiferromagnetically aligned, even without superexchange $J_{1(2)}$, within a large parameter space with nonzero J_H.

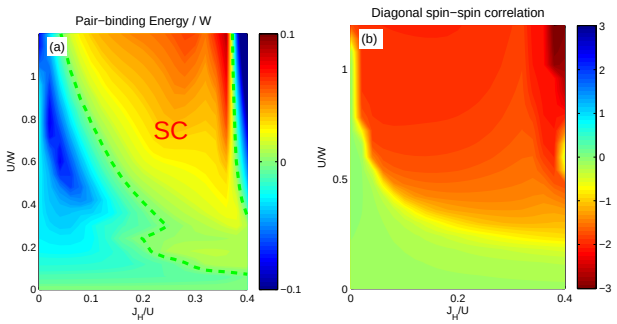

FIG. 4: The pair-binding energy (a) and the diagonal spin-spin correlations (b) for 2×2 plaquette in the three-orbital model are plotted as functions of U/W and J_H/U within exchange coupling $J_2 = 0.1U$. The dotted lines in (a) enclose the regions with positive pair-binding energy, suggesting a SC phase.

B. In presence of J_1 and J_2

We study the two-orbital and three-orbital model with the NN magnetic exchange coupling J_1 and the NNN magnetic exchange coupling J_2. Magnetic exchange coupling J_1 and J_2 drive two different SC phases, which will be discussed respectively in details. Before start, we remark that in the two cases studied, i.e., $J_1 > 0, J_2 = 0$ and $J_1 = 0, J_2 > 0$, the latter may be more relevant in the context of iron-based superconductors. First it is because the NNN pairing is consistent with the $s_\pm$ pairing that is predicted through other methods; second, first principles calculations and inelastic neutron scattering experiments suggest $J_2 > J_1$ in most iron-based SC's; and third, NN pairings (induced by J_1) with A_{1g} symmetry have small and nodal gaps on the hole pockets, in contradiction to the ARPES result.

We summarize the main results for the three-orbital model with superexchange J_2 in Figs. 4, 5, and 6. In Fig. 4, we plot the pair-binding energy and the diagonal (NNN) spin-spin correlation as a function of U/W and J_H/U. With a finite $J_2 = 0.1U$, the SC region is significantly enlarged as well as the NNN-AFM correlation. Additionally, we notice in the same figure that a finite J_H is needed in order to achieve positive pair-binding energy.

The NNN spin-spin correlation decomposed into intra- and inter-orbital components, $\langle Q; \mathrm{GS}|\mathbf{S}^1_\alpha \cdot \mathbf{S}^3_\beta|Q; \mathrm{GS}\rangle$,

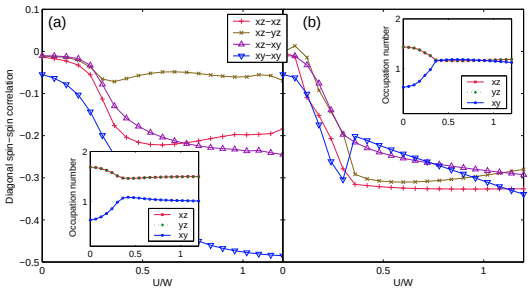

FIG. 5: The orbital-resolved diagonal spin-spin correlations, $\langle \mathbf{S}^1_\alpha \cdot \mathbf{S}^3_\beta \rangle$ $(\alpha, \beta = xz, yz, xy)$, of a 2×2 cluster with 16 electrons (2/3 filling) (a) and 14 electrons (b). The parameters are given by $J_H = 0.2U$, $J_2 = 0.1U$. Insets: The occupation number of different orbitals as a function of U/W with 16 electrons and 14 electrons, respectively.

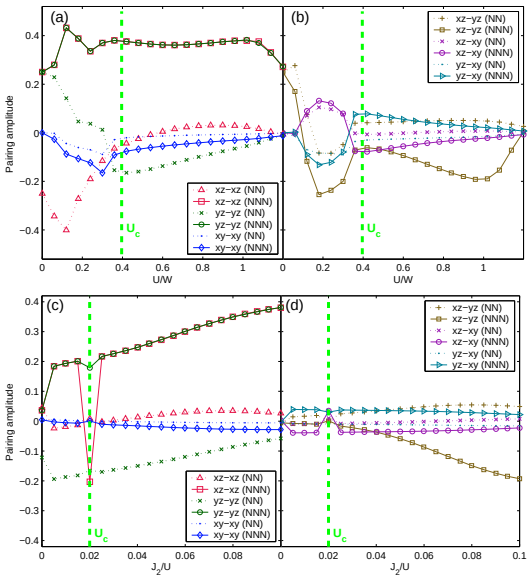

FIG. 6: The pairing amplitude of the intra-orbital [(a)(c)] and the inter-orbital [(b)(d)] electron pairs as function of U [(a)(b)] at fixed parameters of $J_2 = 0.1U$ and $J_H = 0.2U$, and as function of J_2/U [(c)(d)] at fixed parameters of $U = W$ and $J_H = 0.2U$. The 'NN' in the legend means sites 1 and 2 while 'NNN' means sites 1 and 3; all other pairings' amplitude can be derived from the A_{1g} symmetry. Green dotted lines mark the critical U and J_2 right to which the pairing energy is significantly positive.

within a plaquette is shown as a function of U/W in Fig. 5 with fixed $J_H = 0.2U$ and $J_2 = 0.1U$. The NNN-AFM correlation develops when U reaches $\sim 0.4W$ and the intra-orbital correlation is much stronger than the inter-orbital counterpart. Moreover, the d_{xy} orbital has the strongest NNN-AFM correlation because the d_{xy} orbital is half filled [see inset of Fig. 5(a)]. After doping two holes per plaquette, the correlations become almost equal on all three orbitals, as suggested by an equally distributed occupation of three orbitals [see inset of Fig. 5(b)].

The orbital resolved SC pairing amplitudes, defined as $\langle Q = 2; \mathrm{GS}|\Delta_{\alpha\beta}(\mathbf{ij})|Q = 0; \mathrm{GS}\rangle$ with $\Delta_{\alpha\beta}(\mathbf{ij}) = d_{\mathbf{i},\alpha,\downarrow} d_{\mathbf{j},\beta,\uparrow} - d_{\mathbf{i},\alpha,\uparrow} d_{\mathbf{j},\beta,\downarrow}$ are shown in Fig. 6. We find that the pairing is in the A_{1g} channel and such trend is never changed upon increasing J_2 to $0.1U$ (the value we have explored so far). To see this, we can check the eigenvalues of the ground states with $Q = 0$ and $Q = 2$ under symmetry operations of the space group. If they are the same for both states, the order parameter must be even under the symmetry operation, and vice versa. In fact, both states are found invariant under a 90-degree rotation or a mirror reflection about $x = y$ axis. Hence the pairing can only belong to the A_{1g} irreducible representation of the D_{4h} group. Because of the multi-orbital nature, the irreducible representation does not give us complete information as to the pairing structure, but the orbital components as shown in Fig.6 are also needed. The positive pair-binding energy is obtained when $U > U_c \sim 0.4W$, close to where the NNN-AFM develops. The intra-orbital NNN pairings in the $d_{xz(yz)}$ orbitals dominate the pairing strength. The pairing in the d_{xy} orbital is small since the d_{xy} orbital remains half-filled and its AFM correlation is the strongest among all orbitals. However, there is an important feature that the sign of the pairing amplitude on the d_{xy} orbital is opposite to the ones on the $d_{xz(yz)}$ orbitals. We find that the sign-change is as universal as the A_{1g} s-wave pairing symmetry in the whole parameter region we calculate. If one assumes that in going back to the homogeneous limit, the pairing amplitudes within every unit cell are similar to those calculated in the four-site system, we can write down the matrix representation of the pairing in k-space, $\tilde{\Delta}(\mathbf{k})$, defined as $\tilde{\Delta}_{\alpha\beta}(\mathbf{k}) = \langle d_{\alpha\uparrow}(\mathbf{k}) d_{\beta\downarrow}(-\mathbf{k})\rangle$. The matrix representation for the SC phase induced by J_2 interaction is

$$\tilde{\Delta}^{NNN}(\mathbf{k}) = \begin{pmatrix} \Delta_1 & 0 & 0 \\ 0 & \Delta_1 & 0 \\ 0 & 0 & -\Delta_2 \end{pmatrix} \cos k_x \cos k_y, \qquad (3.1)$$

where $\Delta_{1,2}$ are constants and they have the *same* sign. From Fig. 6(c) we also see that the pairing strengths are enhanced by increasing J_2.

For the completeness of the work, we have considered the case with dominant NN AFM exchange J_1, or $J_1 \neq 0, J_2 = 0$. The results, shown in Figs. 7 and 8, for this case are almost parallel to those for $J_1 = 0, J_2 \neq 0$, but one needs to change 'NNN' to 'NN': The region with positive pair binding energy is greatly enlarged when $J_1 = 0.1U$ is included; the region with positive pair binding energy exists within the region with NN AFM spin correlation. And again a finite J_H is needed to obtain positive pair binding energy, or the SC phase. The A_{1g} pairing symmetry has also been confirmed in this case. One can see some deviations from the case with J_2 in the orbital resolved pairing amplitudes shown in Fig. 8. The NN pairing amplitudes are now stronger than their NNN counterparts, which is easily understood because J_1 is a NN AFM coupling. The inter-orbital pairing on d_{xz} and d_{yz} becomes comparable to the dominant intra-orbital pairings on d_{xz} and d_{yz} orbitals. Note that the property,

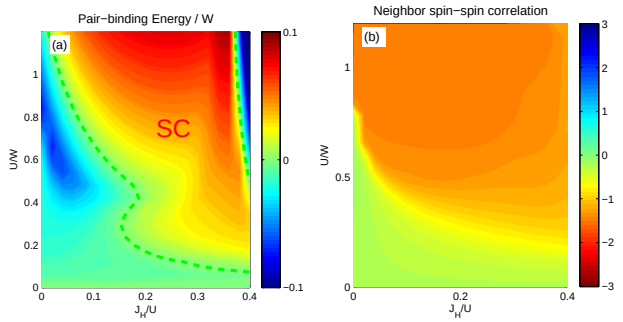

FIG. 7: The pair-binding energy (a) and the NN spin correlations (b) for a 2×2 plaquette in the three-orbital model are plotted as functions of U/W and J_H/U within exchange coupling $J_1 = 0.1U$. The dotted lines in (a) enclose the regions with positive pair-binding energy, suggesting a SC phase.

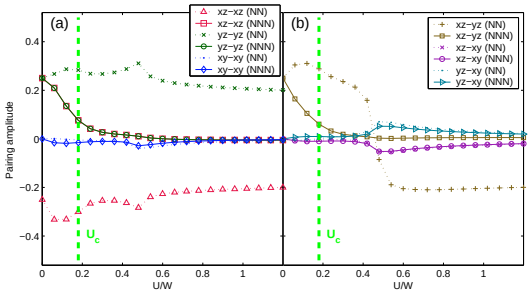

FIG. 8: The pairing amplitude of the intra-orbital (a) and the inter-orbital (b) electron pairings as functions of U at fixed parameters of $J_H = 0.2U$ and $J_1 = 0.1U$. The green dotted lines divide the regions of positive (right) and negative (left) pair-binding energy. The 'NN' in the legend means sites 1 and 2 while 'NNN' means sites 1 and 3; all other pairings' amplitude can be derived from the A_{1g} symmetry.

$\Delta_{\alpha\beta}(\mathbf{12}) = -\Delta_{\alpha\beta}(\mathbf{43})$ with $\alpha = d_{xz}$ and $\beta = d_{yz}$ in a 2×2 plaquette, makes the whole pairing still belonging to the A_{1g} representation. The intra-orbital pairing amplitudes on d_{xz} and d_{yz} orbitals are exactly opposite to each other while the one on d_{xy} orbital is identically zero. This is in a curious consistency with the result from a mean-field theory in a two-band model with J_1-type interaction. If one neglects the inter-orbital pairing we find here, which breaks translational symmetry and could be special due to our artificially modulated lattice, the previously defined pairing matrix in the J_1 induced SC phase is

$$\tilde{\Delta}^{NN}(\mathbf{k}) = \begin{pmatrix} \Delta_3 & 0 & 0 \\ 0 & -\Delta_3 & 0 \\ 0 & 0 & 0 \end{pmatrix} (\cos k_x - \cos k_y), \qquad (3.2)$$

where Δ_3 are constants of comparable magnitude and all smaller pairing channels are ignored. Different from the case with J_2, the pairing magnitude does not change significantly as J_1 increases as far as $J_1 > 0.4W$ (not shown).

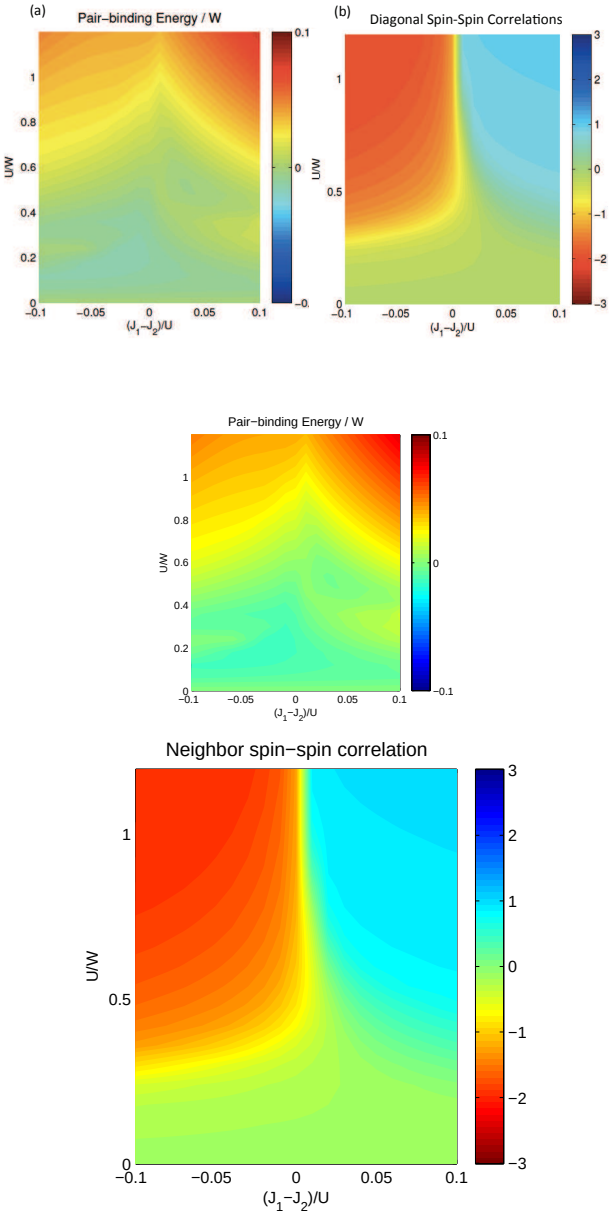

FIG. 9: The pair-binding energy (a) and the diagonal spin-spin correlations (b) for a 2×2 plaquette in the three-orbital model are plotted as functions of U/W and $(J_1 - J_2)/U$ at fixed parameters of $J_H = 0.2U$ and $J_1 + J_2 = 0.1U$.

It is interesting to study the case where both J_1 and J_2 are present. In fact, the SC orders induced by J_1 and J_2 compete with each other. In Fig. 9, we plot the pair-binding energy and the diagonal (NNN) spin-spin correlation function as a function of U/W and $(J_1 - J_2)/U$ keeping $J_1 + J_2 = 0.1U$ and $J_H = 0.2U$. The parameter space can be clearly divided in half by the line $J_1 \sim J_2$. The NNN spin correlations in the two halves are opposite. For $J_1 < J_2$, the NNN exchange is dominant and the NNN correlation is AFM, while for $J_1 > J_2$, the

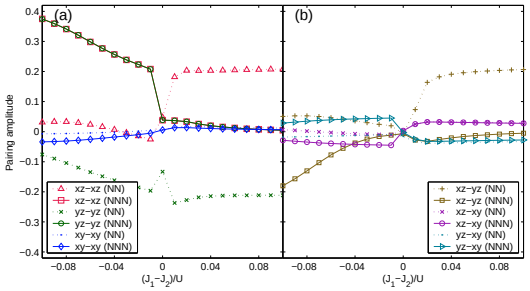

FIG. 10: The pairing amplitude of the intra-orbital (a) and the inter-orbital (b) electron pairs as function of $(J_1 - J_2)/U$ at fixed parameters of $U = W$, $J_H = 0.2U$ and $J_1 + J_2 = 0.1U$. The 'NN' in the legend means sites 1 and 2 while 'NNN' means sites 1 and 3; all other pairings' amplitude can be derived from the A_{1g} symmetry.

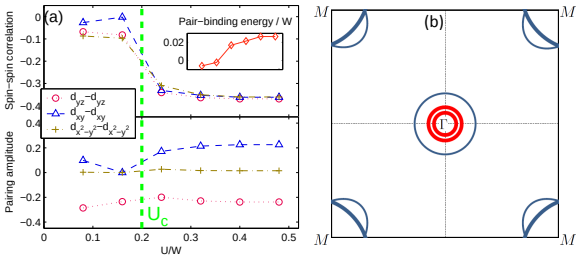

FIG. 11: a: The spin correlation (upper) and pairing amplitude (lower) of diagonal bonds as functions of U in the four-orbital model. The inset shows the pair binding energy in unit of band width. b: The schematic pairing amplitude of a 2D five-orbital model in the superconducting state inside the first (folded) Brillouin zone. Red and blue mean positive and negative signs, and the thickness indicates the size of the gap.

NN spins are antiferromagnetically aligned thus making the NNN spin correlation FM. From this figure one also knows that the SC parameter region shrinks when J_1 and J_2 are close in magnitude. From Fig. 10, one can see that the two SC phases, induced by J_1 and J_2 respectively, are rarely mixed, but there is a sharp divide in between at $J_1 \sim J_2$. We have studied the cases with only J_1 or J_2 present, and one should keep in mind that what applies for $J_1 > 0$, $J_2 = 0$ can be extended to a larger parameter space where $J_1 > J_2 > 0$, and what is true when $J_2 > 0$, $J_1 = 0$ remains valid as far as $J_2 > J_1 > 0$.

IV. ORIGIN OF THE SIGN CHANGED PAIRING ON d_{xy} ORBITAL

There is one singular property of the pairing structure revealed in our results. We find that if J_2 is dominant the pairing amplitude on the d_{xy} orbital is always opposite to those on d_{xz} and d_{yz} orbitals. To check if this property is model dependent, we perform the calculation with a four-orbital model, and find the effect more pronounced: In the four-orbital calculation, the pairing on d_{xy} orbital is as large as that on $d_{xz(yz)}$, but still has the opposite sign (see Fig.11(a)). A simple model in the strong coupling limit can help us understand this effect. Let us consider a two-site system. On each site there is more than one orbital, denoted by $\alpha, \beta, ...$ There are intra- and inter-orbital hoppings between the two sites $t^{12}_{\alpha\beta}$, and the interactions include onsite intra- and inter-orbital Coulomb repulsions U and U'. Suppose there are two electrons, and we know that an effective intra-orbital AFM exchange coupling J is derived from intra-orbital hoppings and intra-orbital repulsion. The AFM exchange obviously favors a singlet pair on the same orbital. Now we consider the effective Josephson coupling between two of these pairs on two different orbitals. A singlet state formed on the αth orbital is $|s_\alpha\rangle = (c^\dagger_{1\alpha\uparrow}c^\dagger_{2\alpha\downarrow} - c^\dagger_{1\alpha\downarrow}c^\dagger_{2\alpha\uparrow})|0\rangle/\sqrt{2}$. We also define a doubly occupied state that will be used as a intermediate state: $|d\rangle = (c^\dagger_{1\beta\uparrow}c^\dagger_{1\alpha\downarrow} - c^\dagger_{1\beta\downarrow}c^\dagger_{1\alpha\uparrow} + c^\dagger_{2\beta\uparrow}c^\dagger_{2\alpha\downarrow} - c^\dagger_{2\beta\downarrow}c^\dagger_{2\alpha\uparrow})|0\rangle/2$. Treating the inter-orbital hoppings as perturbation, i.e., $t^{12}_{\alpha\beta} \ll U'$, the first order correction to the ground state $|s_\alpha\rangle$ is

$$|s'_\alpha\rangle = \frac{|s_\alpha\rangle + \sum_{\beta\neq\alpha} \sqrt{2}\frac{t^{12}_{\alpha\beta}}{\epsilon_\alpha - \epsilon_\beta - U'}|d\rangle}{\sqrt{1 + 2(\frac{t^{12}_{\alpha\beta}}{\epsilon_\alpha - \epsilon_\beta - U'})^2}}. \tag{4.1}$$

In this new basis $|s'_\alpha\rangle$, the pair hopping amplitude between a pair on orbital α and another on orbital β is (assuming $\epsilon_\alpha \sim \epsilon_\beta$)

$$\langle s'_\alpha|H|s'_\beta\rangle = -2\frac{t^{12}_{\alpha\beta}t^{12}_{\beta\alpha}}{U'}. \tag{4.2}$$

Or we can write the effective Hamiltonian in the singlet pair subspace as

$$H^{eff} = -2\frac{t^{12}_{\alpha\beta}t^{12}_{\beta\alpha}}{U'}\Delta^\dagger_\alpha\Delta_\beta, \tag{4.3}$$

where $\Delta^\dagger_\alpha$ creates a single pair $|s'_\alpha\rangle$. In the case of iron-SCs, the general symmetry of the lattice requires $t^{\mathbf{ij}}_{xz,yz} = t^{\mathbf{ij}}_{yz,xz}$ and $t^{\mathbf{ij}}_{xy,xz(yz)} = -t^{\mathbf{ij}}_{xz(yz),xy}$, as sketched in Fig. 1. Thus the Josephson coupling between the xz and yz is negative while the one between the $xz(yz)$ and xy is positive, which favors the sign change between $\Delta_{xz(yz),xz(yz)}(\mathbf{ij})$ and $\Delta_{xy,xy}(\mathbf{ij})$. This explains the sign change observed in our numerical results. The actual value of this Josephson coupling is determined by details of the model, but the sign is only determined by lattice symmetry and hence model independent.

V. DISCUSSION

Strictly speaking, the results we obtained apply to the strong coupling limit in which electron-electron correlation is comparable to hopping parameters. However,

they are consistent with the results of many previous studies[2,4,12,13], using other models and methods. The pairing symmetry is dominated by the A_{1g} channel. The pairing strength is drastically enhanced when AFM J_1 or J_2 is included. When J_2 is larger than J_1, the A_{1g} pairing will have the sign change between electron and hole pockets (so called $s_{\pm}$-wave). However, when J_1 is much larger than J_2, the A_{1g} pairing will be a nodal d-wave with nodes on hole pockets at Γ.

Our study also suggests that the Hund's coupling is very important in inducing the SC pairing and the AFM correlation[7]. Without the Hund's coupling, the model does not have positive pair-binding energy in reasonable parameter regions of other interaction parameters.

Our result indicates that the d_{xy} orbital is extremely important in the strong coupling limit. The pairing in the d_{xy} orbital favors an opposite sign to those in the d_{yz} and d_{xz} orbitals when J_2 dominates the pairing. This relation, if still holds in the homogeneous limit, will result in the sign change between the hole pockets at Γ which have $d_{yz,xz}$ orbital character and the hole pocket at M in unfolded Brillouin zone which has d_{xy} orbital character[39], a result can be tested explicitly in future experiments. A schematic plot of this prediction in folded Brillouin zone is shown in Fig. 11(b).

Finally, we want to point out that the time reversal symmetry breaking suggested in Refs. 37,38 is not favored in our study. A time reversal symmetry breaking SC state is favored only if the Josephson couplings between all three orbitals are positive. However, in Eq. (4.3), one of the three Josephson couplings has opposite sign to the other two.

VI. CONCLUSION

Our study on the checkerboard models constructed from the two-, three- and four-orbitals for iron-SCs confirms the robustness of A_{1g} pairing and suggests new orbital dependence of the pairing amplitude. We use ED to solve the models in the weak inter-plaquette coupling limit. We find that in the reasonable parameter region, the pairing symmetry always belongs to the A_{1g} irreducible representation of the D_{4h} space group. With a moderate NNN exchange coupling $J_2 \sim 0.1U$, the pairing is consistent with a gap of the functional form $\cos k_x \cos k_y$, or the $s_{\pm}$-wave in a homogeneous system. In the orbital resolved pairing structure, the amplitude on d_{xy} orbital is always opposite to that on $d_{xz(yz)}$ in three- and four-orbital models. We explain this feature in the context of the inherent symmetry of hopping parameters and the strong coupling nature of our model. Experimental consequences of this finding are discussed.

We thank A. B. Bernevig, S. Kivelson, H. Ding, D.L. Feng, X.H. Chen and P.C. Dai for help in discussion. JPH thanks E. Demler for asking question related to this study. JP is supported by National Basic Research (973) Program of China (grants No. 2012CB821400), National Science Fundation of China (NSFC-11190024). WFT is supported by the NSC in Taiwan under Grant No. 100-2112-M-110-001-MY2. YJJ acknowledge the support from NSF, Zhejiang (No.Y7080383) and NSF, China (No.11004174).

* Corresponding author; Electronic address: hu4@purdue.edu

[1] Y. Kamihara, T. Watanabe, M. Hirano, and H. Hosono, J. Am. Chem. Soc. **130**, 3296 (2008).
[2] K. Seo, B. A. Bernevig, and J. Hu, Phys. Rev. Lett. **101**, 206404 (2008).
[3] Q. Si and E. Abrahams, Phys. Rev. Lett. **101**, 076401 (2008).
[4] E. Berg, S. A. Kivelson, and D. J. Scalapino, Phys. Rev. B **81**, 172504 (2010).
[5] C. Fang, H. Yao, W.-F. Tsai, J. Hu, and S. A. Kivelson, Phys. Rev. B **77**, 224509 (2008).
[6] C. Xu, M. Mueller, and S. Sachdev, Phys. Rev. B **78**, 02051 (2008).
[7] K. Haule and G. Kotliar, New J. Phys. **11**, 025021 (2009).
[8] K. Haule, J. H. Shim, and G. Kotliar, Phys. Rev. Lett. **100**, 226402 (2008).
[9] J. Dai, Q. Si, J.-X. Zhu, and E. Abrahams, PNAS **106**, 4118 (2009).
[10] I. I. Mazin, D. J. Singh, M. D. Johannes, and M. H. Du, Phys. Rev. Lett. **101**, 057003 (2008).
[11] K. Kuroki, S. Onari, R. Arita, H. Usui, Y. Tanaka, H. Kontani, and H. Aoki, Phys. Rev. Lett. **101**, 087004 (2008).
[12] F. Wang, H. Zhai, Y. Ran, A. Vishwanath, and D.-H. Lee, Phys. Rev. Lett. **102**, 1047005 (2009).
[13] R. Thomale, C. Platt, W. Hanke, and B. A. Bernevig, Phys. Rev. Lett. **106**, 187003 (2011).
[14] V. Cvetkovic and Z. Tesanovic, Europhys. Lett. **85**, 37002 (2009).
[15] M. M. Korshunov and I. Eremin, Phys. Rev. B **78**, 140509 (2008).
[16] A. V. Chubukov, D. V. Efremov, and I. Eremin, Phys. Rev. B **78**, 134512 (2008).
[17] D. J. Scalapino, Phys. Rep. **250**, 329 (1995).
[18] D. J. Scalapino and S. A. Trugman, Philos. Mag. B **74**, 607 (1996).
[19] W.-F. Tsai and S. A. Kivelson, Phys. Rev. B **73**, 214510 (2006).
[20] H. Yao, W.-F. Tsai, and S. A. Kivelson, Phys. Rev. B **76**, 161104(R) (2007).
[21] E. Altman and A. Auerbach, Phys. Rev. B **65**, 104508 (2002).
[22] R. Thomale, C. Platt, W. Hanke, J. Hu, and B. A. Bernevig, arXiv:1101.3593 (2011).
[23] Y.-Z. You, H. Yao, and D.-H. Lee, arXiv:1103.3884 .
[24] T. A. Maier, S. Graser, P. J. Hirschfeld, and D. J. Scalapino, arXiv:1101.4988 (2011).
[25] C. de la Cruz, Q. Huang, J. W. Lynn, Jiying Li, W. Ratcliff II, J. L. Zarestky, H. A. Mook, G. F. Chen, J. L. Luo, N. L. Wang, and Pengcheng Dai, Nature **453**, 899 (2008).

[26] J. Zhao, D. T. Adroja, D.-X. Yao, R. Bewley, S. Li, X. F. Wang, G. Wu, X. H. Chen, J. Hu, and P. Dai, Nature Physics **5**, 55 (2009).
[27] J. Zhao, D.-X. Yao, S. Li, T. Hong, Y. Chen, S. Chang, W. Ratcliff II, J. W. Lynn, H. A. Mook, G. F. Chen, J. L. Luo, N. L. Wang, E. W. Carlson, J. Hu, and P. Dai, Phys. Rev. Lett. **101**, 167203 (2008).
[28] H. Ding, P. Richard, K. Nakayama, T. Sugawara, T. Arakane, Y. Sekiba, A. Takayama, S. Souma, T. Sato, T. Takahashi, Z. Wang, X. Dai, Z. Fang, G. F. Chen, J. L. Luo, N. L. Wang, Europhys. Lett. **83**, 47001 (2008).
[29] Y. Zhang, L. X. Yang, F. Chen, B. Zhou, X. F. Wang, X. H. Chen, M. Arita, K. Shimada, H. Namatame, M. Taniguchi, J. Hu, B. P. Xie, and D. L. Feng, Phys. Rev. Lett. **105**, 117003 (2010).
[30] K. Nakayama, T. Sato, P. Richard, Y.-M. Xu, T. Kawahara, K. Umezawa, T. Qian, M. Neupane, G. F. Chen, H. Ding, and T. Takahashi, Phys. Rev. B **83**, 020501(R) (2011).
[31] J. Guo, S. Jin, G. Wang, S. Wang, K. Zhu, T. Zhou, M. He, and X. Chen, Phy. Rev. B. **82**, 180520 (2010).
[32] S. Raghu, X.-L. Qi, C.-X. Liu, D. Scalapino, and S.-C. Zhang, Phys. Rev. B **77**, 22503 (2008).
[33] M. Daghofer, A. Nicholson, A. Moreo, and E. Dagotto, Phys. Rev. B **81**, 014511 (2010).
[34] M. Daghofer, A. Moreo, J. A. Riera, E. Arrigoni, D. J. Scalapino, and E. Dagotto, Phys. Rev. Lett **101**, 237004 (2008).
[35] D. Fisher and P. C. Hohenberg, Phys. Rev. B **37**, 493 (1988).
[36] P. A. Lee and X.-G. Wen, Phys. Rev. B **78**, 144517 (2008).
[37] W. C. Lee, S. C. Zhang, and C. Wu, Phys. Rev. Lett **102**, 217002 (2009).
[38] P. Goswami, P. Nikolic, and Q. Si , Europhys. Lett. **91**, 37006 (2010).
[39] Y. Zhang, F. Chen, C. He, B. Zhou, B. P. Xie, C. Fang, W. F. Tsai, X. H. Chen, H. Hayashi, J. Jiang, H. Iwasawa, K. Shimada, H. Namatame, M. Taniguchi, J. P. Hu, and D. L. Feng, Phys. Rev. B **83**, 054510 (2011).